

Workspace and Dexterity Analyses of Hexaslide Machine Tools

A.B.Koteswara Rao
Dept. of Mechanical Engineering
Indian Institute of Technology Delhi
Hauz Khas, New Delhi-110 016
India
abh_iitd@yahoo.co.in

P.V.M.Rao'
Dept. of Mechanical Engineering
Indian Institute of Technology Delhi
Hauz Khas, New Delhi-110 016
India
pvmrao@mech.iitd.emet.in

S.K.Saha
Dept. of Mechanical Engineering
Indian Institute of Technology Delhi
Hauz Khas, New Delhi-110 016
India
saha@mech.iitd.ernet.in

Abstract - This paper presents kinematic analysis of B class of parallel manipulators, namely, Hexaslides, for machine tool applications. Hexaslides have constant-length legs. The inverse and direct kinematics solutions, to study the workspace properties of hexaslides are presented. Various kinematic performance indices, namely, workspace volume, workspace volume index i.e., the ratio of workspace volume to machine size and global dexterity index of hexaslides having same foot print size are used to study different rail-arrangements. Secondly, effect of two important parameters related to configuration, i.e., gap between adjacent rails in case of hexaglide configuration and inclination of rails in case of slanted configuration, on the performance measures is presented.

1. INTRODUCTION

Machine tools with parallel mechanisms, in which every axis is a direct link between the tool or mobile platform and fixed platform of the machine, unlike that in case of conventional serial machine tools where there exists a serial arrangement of feed axes and each axis has to carry load and moves the weight of all the following axes, meet the requirement of high dynamic performance, i.e., high stiffness constructions with little moving masses. Stewart platform [1] and the tyre test machine [2] are initial works in the area of parallel kinematic machines (PKMs). The machine tools based on parallel kinematic structures are reported in [3-61].

Parallel kinematic structures are made-up of one or more closed kinematic chains, whose end effector represents tool platform with several degree of freedom (d.o.f) with respect to fixed platform. Guide chains coupling the two platforms can be moved independent to each other. One end of each guide chain, called shut, is coupled to the fixed platform while the other end is coupled to the tool platform by means of a suitable joint. Each joint allows several d.o.f. As there is no bending of legs, all axes simply have traction or compression forces. They are reconfigurable and can be built with relatively low investment as many of its components consist of standard machine elements.

Most common versions of PKMs, with six legs offering six-d.o.f., are Hexapods and Hexaslides. The hexaslides, based on the design chosen for feed drives, consist of six constant-length legs. The positions of the base joints, of the legs, on their respective rail-axes control the posture of the

mobile platform in space. As the main moving parts, i.e., legs, can be made light but stiff, these find applications in machining, measuring, and handling etc. with high accuracy and precision. The Hexaslide machine tools (HSMs) require better workspace properties. Complex workspace is one of the major drawbacks of these HSMs. Moreover, the Jacobian matrix, J , which relates the joint rates to the output velocities, is not constant and not isotropic; the performances vary considerably for different points in the workspace and for different directions at one given point. This is a serious drawback for machining applications [6-81]. Hence in the design of HSMs, shape and size of the workspace, workspace volume index i.e., the ratio of workspace volume to machine size, dexterity, etc., are considered as the most important performance indices.

Out of the parameters that influence the performance of HSMs such as rail-arrangement, actuator stroke, leg-lengths, ranges of tool platform joints and double revolute joints; effect of rail-arrangement is the main concern in this work.

2. HEXASLIDE MACHINE TOOLS

A general hexaslide based machine tool consists of six distinct rails as shown in Fig. 1. The sliders move along their rails, whereas the legs of constant length are connected to the sliders through Revolute-Revolute joints. Other end of each leg is connected to the tool or mobile platform through spherical joints. Actuation of the sliders on their respective rails drives the tool platform in space.

There are primarily three machine tools based on hexaslides, namely, 1) Hexaglide [3], developed at ETH

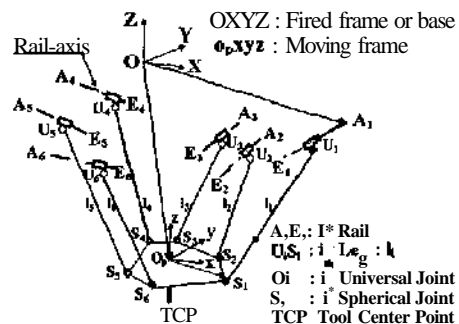


Fig. 1 The general hexaslide machine tool

* Corresponding author

Zurich, consisting of coplanar and parallel rails as shown in Fig 2(a); 2) HexaM (41 developed by Toyoda consisting of slanted rails as shown in Fig 2(h) and 3) Linapod [5] developed at University of Stuttgart, which has the rails arranged in vertical direction as shown in Fig 2(c). These are all based on simple scissor drives [SI and the only difference is their rail-arrangement. The TIARA hexapod [9] with constant-length struts, consist of its rails resembling a tiara.

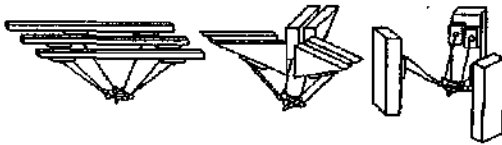


Fig. 2(a) Hexaglide Fig. 2(b) HenaM Fig. 2(c) Linapod
(courtesy: hnp:11~bot.gmc.ulavalcai-bonevn

The workspace analysis of a general HSM based on vertex space concept [IO] was proposed. Adopting a geometric algorithm, the volume and shape of the workspace at a given orientation, and their variation with orientation were discussed. Alternatively, a parameterized model [II] that applies to hexapods with fixed-length legs was developed to find the workspace and dexterity. However, there is no effort made to find the optimum rail angle. Moreover, the dexterity analysis was based on the variation in the singular values of the corresponding Jacobian matrix. The three different versions of HSMs, considered for comparison, consist of rails parallel by pairs only.

In regards to the indices of manipulator dexterity, the condition number μ , given by $\mu = a_{max} / a_{min}$ where a_{max} and a_{min} are the largest and smallest singular values of the J , was used in [12]. Geometrically, the associated Jacobian matrix J describes a hyperellipsoid having lengths defined by its singular values. The determinant of this Jacobian matrix, $\det(J)$ is proportional to the volume of hyperellipsoid. The condition number represents the sphericity of the hyperellipsoid. The manipulability measure [13] w , given by

$$w = \sigma_1 \sigma_2 \sigma_3 \sigma_4 \sigma_5 \sigma_6 = \sqrt{J \det(J^T J)}$$

was defined to describe the ability of manipulator to change its position and direction in its workspace. The conditioning of J and the manipulability ellipsoid associated with J were used to optimize the workspace shape and performance uniformity of the Orthoglide 1141. Alternatively, global performance indices, that consider the dexterity of the manipulator over the entire workspace, were used in [15], 1161.

For any practical purposes, prior to the development of any HSM with constant-length struts, it is necessary to identify a suitable arrangement of rails i.e., (i) either paired or unpaired rails, and (ii) orientation of the rails that fulfill the desired performances. Since no such data is readily available in the literature, a comparison among HSMs with different rail-arrangements related to various kinematic performance indices, namely, workspace volume, workspace volume index, and global dexterity index of the hexaslides having same foot print size but with different rail-arrangements, has

been carried-out in this work. Effect of gap between adjacent rails and inclination angle of the rails on workspace and dexterity are also reported.

3. KINEMATIC ANALYSIS

The degree-of-freedom for a generalized HSM can be found, using the Kutzbach criterion [17], as 6. For the kinematic analysis of the generic model of HSM, consider the loop $O A_i U_i S_i O$ in Fig. 3, in which O -XYZ : Fixed frame of reference attached to the base, O_i -xyz : Moving frame attached to the tool platform, $p = O O_i = [p_x, p_y, p_z]^T$, the position of center of the moving platform O_i , in fixed frame and $[R]$ is the Rotation matrix representing the orientation of the moving frame, O_i -xyz, with reference to O -XYZ.

for $i=1$ to 6,
 U_i is the unit vector along the P rail in fixed frame; d_i is the distance of the J^* actuator from A_i ; $a_i = O A_i$, in fixed frame; $d_i = A_i U_i$, in fixed frame; $l_i = U_i \&$ in fixed frame; $s_i = A_i S_i$, in fixed frame; $b_i = O_i P_{S_i}$, in moving frame.

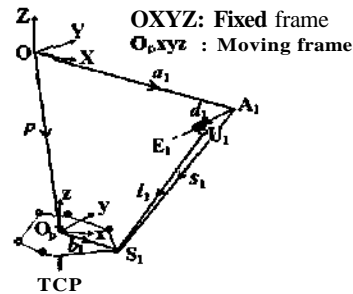


Fig. 3 Kinematic chain of HSM

3.1 Position Analysis

From the geometry, s_i can be written as,

$$s_i = p + [R]b_i - n_i = d_i + l_i, \text{ for } i=1 \text{ to } 6 \quad (1)$$

Since $d_i = d u_i$, (1) can be written as,

$$d u_i = p + [R]b_i - U_i - l_i \quad (2)$$

$$\text{or } (p + [R]b_i - U_i - l_i) \cdot d u_i = 0 \quad (3)$$

The inverse kinematic problem can then be solved to find d_i using (3), while p and $[R]$ are given. Equation (3) is quadratic in d_i . There exists two solutions $d_i^{(1)}$, $d_i^{(2)}$. The true solution can be found based on the motion continuity. Alternatively, it can be shown that d_i is given by

$$d_i = u_i \cdot s_i \pm \sqrt{l_i^2 - [s_i \cdot \{ \dots \}]}, \text{ for } i=1 \text{ to } 6 \quad (4)$$

Equation (4) also offers two values $d_i^{(1)}$, $d_i^{(2)}$. The true solution can be identified based on the motion continuity. The given pose is said to be achievable by the tool platform if the values of d_i satisfy the constraint

$$0 \leq d_i \leq r_i \quad (5)$$

along with the constraints imposed due to range of motion allowed by universal and spherical joints for all $i=1$ to 6, where r_i is the length of the i th rail.

To solve the forward kinematics, i.e., to find p and $[RI]$ for given d_i , consider (3) in the following form:

$$f_i(\mathbf{x}) = (\mathbf{q}_i)^T (\mathbf{q}_i) - l_i^2 = 0 \quad (6)$$

$$\text{where } \mathbf{q}_i = p + [R]b_i - U_i - d_i \quad (7)$$

For the HSM with the known geometry, i.e., U_i , and b_i , and given the values of d_i , (6) gives six scalar non-linear, simultaneous equations in terms of the unknown vector $\mathbf{x} = [p_x, p_y, p_z]^T$. As p_x, p_y , and p_z are the three Cartesian coordinates of the tool, and ϕ, θ, ψ are the ZYZ Euler angles [15], \mathbf{x} represents pose vector of the tool platform. As (6) will not give closed-form solution, Newton-Raphson method [9], can be used.

3.2 Velocity Analysis

The time derivative of (2) yields,

$$\dot{d}_i \mathbf{u}_i = \mathbf{v} + \mathbf{w} \times [RI] b_i - W_i \mathbf{x}_i \quad (8)$$

where \dot{d}_i is the vector of actuator speeds, \mathbf{v} and \mathbf{w} are the linear and angular velocities of the moving platform, and W_i is the angular velocity of the i th leg. Taking the dot product of \mathbf{u}_i on the both sides of (8), we get

$$\dot{d}_i \mathbf{u}_i^T \mathbf{u}_i = [\mathbf{v} + \mathbf{w} \times [R] b_i]^T \mathbf{u}_i \quad (9)$$

Equation (9) may be represented in the matrix form as,

$$J_i \dot{d}_i = J_i \dot{\mathbf{x}} \quad (10)$$

where $\dot{\mathbf{x}} = [\dot{p}_x, \dot{p}_y, \dot{p}_z, \dot{\phi}, \dot{\theta}, \dot{\psi}]^T$: vector of the end effector velocity; $\dot{d}_i = [\dot{d}_1, \dots, \dot{d}_6]^T$, the vector of actuator rates or speeds, $J_i = \text{diag}(\mathbf{u}_i^T \mathbf{u}_i, \dots, \mathbf{u}_i^T \mathbf{u}_i)$, which is a 6x6 matrix and J_i is given by,

$$J_i = \begin{bmatrix} \mathbf{u}_i^T & ([R] b_i \times \mathbf{u}_i)^T \\ \vdots & \vdots \\ \mathbf{u}_i^T & ([R] b_i \times \mathbf{u}_i)^T \end{bmatrix}_{6 \times 6}$$

Equation (10) may be re-written as

$$\dot{d}_i = J_i \dot{\mathbf{x}} \quad (11)$$

where J_i is the Jacobian matrix of the tool platform and is given by, $J_i = J_i^T J_i$. If J_i becomes singular for a certain position and orientation of the tool platform within the workspace of HSM, i.e., when $\mathbf{u}_i^T \mathbf{u}_i = 0$, for any $i=1$ to 6; it corresponds to the *stationary singularity* i.e., the leg standing perpendicular to the rail. In this case of singularity, the HSM loses one or more d.o.f. When J_i becomes singular, which corresponds to the *uncertainty singularity*, the HSM gains one or more d.o.f. Taking the time derivative of (8), acceleration analysis may also be done. As this analysis is not required for the present work, it is not presented.

4. PERFORMANCE MEASURES

In the design of HSMs, much concern is given to the shape and size of the workspace, ratio of workspace volume to machine size, dexterity etc., which are presented next.

4.1 Workspace Volume (WSV)

The complete or total workspace of a HSM is a six dimensional space for which complete graphical representation is very difficult to obtain. Out of different types of subsets of the complete workspace [19], the most commonly determined workspace is the constant-orientation workspace, which is a three-dimensional space or volume reachable by center of the tool platform (or the TCP) while orientation is constant. For the workspace evaluation, a search method [20], based on the inverse kinematics, is applied. Search proceeds by defining a bounding box covering a maximum possible reachable space of HSM, and then slicing the bounding box into a number of layers with each layer is being discretized into points. For each of these points the distance, d_i in Fig.3 is calculated and the constraints are checked. If the constraints are not violated, the point under computation is considered within the workspace, otherwise considered outside of the workspace. The workspace volume is defined as,

$$WSV = Z A, h \quad (12)$$

where A is the reachable area in the m th layer, and h is the layer interval.

4.2 Workspace Volume Index (WVI)

The workspace volume index is the ratio of workspace volume to the size of HSM. Size of HSM is taken as the product of area of the fixed platform and the maximum reach of the TCP in Z-direction.

4.3 Global Dexterity Index (GDI)

Dexterity is a measure of kinematic performance of HSMs. It depicts the ability to arbitrarily change its position and orientation, or apply forces and torques in arbitrary directions during machining. The Global Dexterity Index [15] is given by

$$GDI = \frac{\int \left(\frac{1}{K} \right) dW}{\int dW} \quad (13)$$

where dW is an infinitesimal small element representing one of the workspace points and K is the condition number of the Jacobian at that point. It represents the uniformity of manipulability within the entire workspace. In the present work, for the comparison of HSMs, GDI using (13) is used with, $K = \|\mathbf{j}\| / \|\mathbf{j} \cdot \mathbf{j}\|$, where $\|\cdot\|$ refers to the 2-norm,

5. COMPARISON OF HSMs

A program has been developed in MATLAB to model a generic HSM configuration and to determine shape and size of the workspace, range of moving platform, workspace volume index and the global dexterity index. The results obtained from the program are verified by finding the workspace volume for certain known cases. One such validation involves finding workspace of a *Test machine*, shown in Fig. 4(a), with following details.

5.1 Test Machine and its Workspace

Fixed platform ; Regular hexagon of side 500 units
 Moving platform : Regular hexagon of side 100 units
 Legs : 6 Nos of each 400 units length
 Rails : 6 Nos of each 250 units length
 Rails are arranged vertically through the vertices of fixed platform. For this test machine, the workspace would be just a vertical line as the tool tip traces a straight-line and all these points would be singular points suffering from the stationary singularity. The workspace plot, obtained from the program is shown in Fig. 4(b).

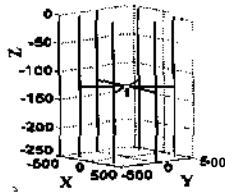


Fig. 4(a) Test machine

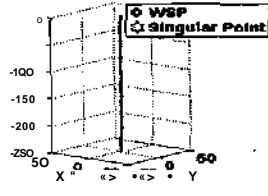


Fig. 4(b) Workspace and singular points

5.2 Configurations of HSM considered for Comparison

The performance indices of HSMs having different rail-arrangements have been evaluated. Results for some typical cases, which also include most of the rail-arrangements proposed by researchers in the past, have been presented. These configurations shown in Fig. 5(a) to Fig. 5(g) are as follows:

HSM with Radial rails: All the rail-axes are radial and are symmetric with Z-axis as shown in Fig. 5(a)

HSM with Radial rails parallel by pairs: The rail-axes are parallel by pairs, the pairs being radial and symmetric with Z-axis as shown in Fig. 5(b)

HSM with Slanted rails: All the rail-axes are slanted and symmetric with Z-axis as shown in Fig. 5(c)

HSM with Slanted rails parallel by pairs: The rail-axes are slanted, parallel by pairs, the pairs being symmetric with Z-axis as shown in Fig. 5(d)

HSM with Vertical rails: All the rail-axes are vertical and symmetric with Z-axis as shown in Fig. 5(e)

HSM with Vertical rails parallel by pairs: The rail-axes are vertical, parallel by pairs, the pairs being symmetric with Z-axis as shown in Fig. 5(f)

HSM with rails parallel, coplanar: Hexaglide - Fig. 5(g).

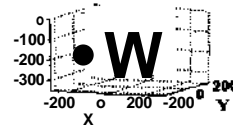


Fig. 5(a) Radial rails

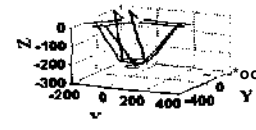


Fig. 5(b) Radial rails parallel by pairs

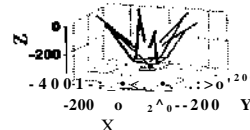


Fig. 5(c) Slanted rails

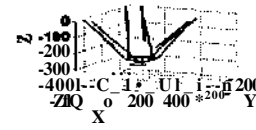


Fig. 5(d) Slanted rails parallel by pairs

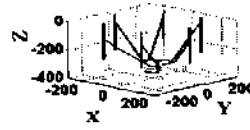


Fig. 5(e) Vertical rails

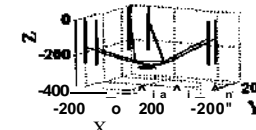


Fig. 5(f) Vertical rails parallel by pairs

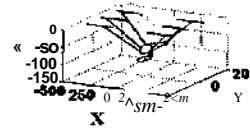


Fig. 5(g) Hexaglide

Fig 5(a)-(g) HSMs with different rail-arrangements

For the purpose of comparison, same sized fixed platform, same sized moving platform and same actuator stroke i.e., lengths of rails are used for all configurations. Fixed platform is a regular hexagon of side 0.255m for the HSM shown in Fig. 5(a), (c) and (e). It is a hexagon, for the HSM having rails parallel by pairs, with long and short sides equal to 0.5m and 0.08m, respectively. For the hexaglide configuration shown in Fig. 5(g), it is a rectangle. The gap between adjacent rails (G) and position of rails are considered such that the area of this rectangle is same as that of fixed platform in other cases. Tool platform is taken as a hexagon, for all HSMs, with long and short sides equal to 0.141m and 0.052m, respectively. Length of each rail is taken as 0.2501 and length of each leg is taken as 0.3m for all cases of study.

As the first three columns of Jacobian matrix i.e., J in (11) are dimensionless while the last three columns have units of length, in order to analyze the global dexterity index independent of the physical size, the last three columns are divided by the distance between center of the tool platform and the center of the spherical joint on the tool platform.

The performance indices, workspace volume, workspace volume index, global dexterity index and range of TCP in X-direction (R_x), in Y-direction (R_y) and in Z-direction (R_z), for HSMs with different rail-arrangements, considering the HSM with its tool platform at constant-orientation i.e., horizontal only, are presented in Table I. It can be observed from Table I that maximum workspace volume is offered by the HSM having slanted configuration with paired rails.

Comparison of the performance indices in case of hexaglide configuration for different gaps between adjacent rails is given in Table 2. It may be noted that Hexaglides 1, 2, 3, and 4 have same area of the fixed platform, which is a rectangle.

TABLE 1
PERFORMANCE INDICES FOR DIFFERENT VERSIONS OF HSMs

Rx, m	Ry, m	Rz, m	WSV, m ³	WVr	GDI
HSM with Radial rails					
0.14	0.14	0.04	0.00028	0.006	0.057
HSM with Slanted rails (48°)					
0.44	0.44	0.22	0.01624	0.205	0.069
HSM with Vertical rails					
0.22	0.21	0.22	0.00385	0.049	0.083
HSM with Radial rails parallel by pairs, G = 0.080m					
0.32	0.36	0.11	0.00214	0.044	0.215
HSM with Slanted rails parallel by pairs (43°), G = 0.080m					
0.45	0.44	0.25	0.01797	0.231	0.257
HSM with Vertical rails parallel by pairs, G = 0.080m					
0.13	0.14	0.24	0.00183	0.026	0.291
Hexaglide, G = 0.102m (which offers maximum WSV)					
0.17	0.40	0.24	0.00931	0.230	0.034

TABLE 2
VARIATION IN PERFORMANCE INDICES WITH THE GAP BETWEEN ADJACENT RAILS FOR HEXAGLIDE

	WSV, m ³	WVI	GDI
Hexaglide-1: G = 0.080m	0.00049	0.029	0.018
Hexaglide-2: G = 0.085m	0.00264	0.098	0.025
Hexaglide-3: G = 0.102m	0.00931	0.230	0.034
Hexaglide-4: G = 0.168m	0.00011	0.002	0.021

Variation of performance indices of HSM with slanted configuration, having paired rails, and having unpaired rails, with the inclination of the rails with horizontal (ρ) have been computed and compared in Tables 3 and 4 respectively. Variation of WSV and GDI with the inclination of the rails is shown in Fig 6(a) and Fig. 6(b) respectively. Due to the space limitation, Shapes of workspaces of some salient HSMs having rails parallel by pairs only are shown in Fig. 7(a-d). In these plots, WSP and ICP correspond to the Workspace Points and Ill-Conditioned Points respectively. The reachable points, for which the condition number of the Jacobian matrix is more than 50, are considered as Ill-conditioned points.

TABLE 3
PERFORMANCE INDICES FOR DIFFERENT RAIL INCLINATION (RAILS PARALLEL BY PAIRS)

P.deg	Rx, m	Ry, m	Rz, m	WSV, m ³	GDI
0	0.32	0.36	0.11	0.00214	0.215
22.5	0.46	0.48	0.21	0.01188	0.183
43	0.45	0.44	0.25	0.01797	0.257
67.5	0.32	0.30	0.31	0.01097	0.335
90	0.13	0.14	0.24	0.00183	0.291

TABLE 4
PERFORMANCE INDICES FOR DIFFERENT RAIL INCLINATION (RAILS UNPAIRED)

P.deg	Rx, m	Ry, m	Rz, m	WSV, m ³	GDI
0	0.14	0.14	0.04	0.00028	0.057
22.5	0.33	0.33	0.12	0.00394	0.042
45	0.44	0.44	0.22	0.01624	0.069
67.5	0.36	0.37	0.25	0.01302	0.101
90	0.22	0.21	0.22	0.00385	0.083

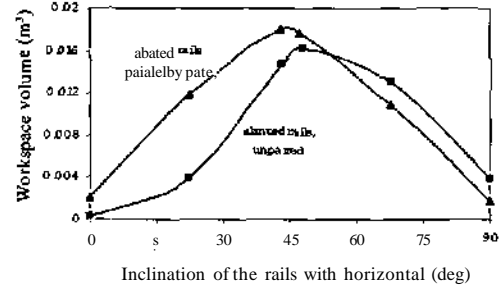


Fig. 6(a) Variation of workspace with the rail inclination

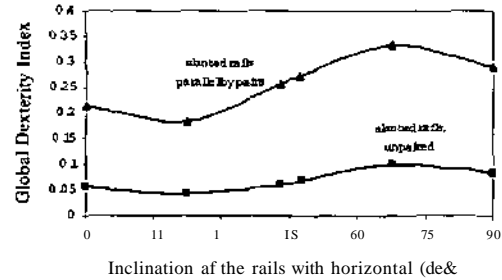


Fig. 6(b) Variation of GDI with the rail inclination

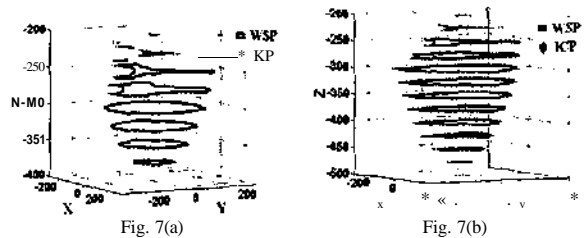


Fig. 7(a)

Fig. 7(b)

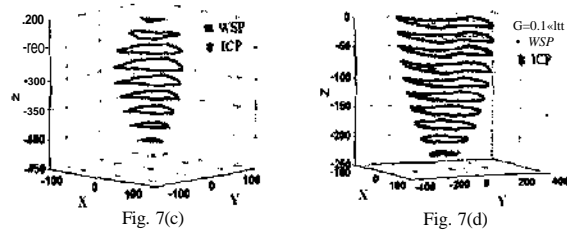


Fig. 7(c)

Fig. 7(d)

Fig. 7(a)-(d) Workspace plots of different HSMs (a) for HSM-paired rails, $\rho = 22.5^\circ$, (b) for HSM-paired rails, $\rho = 67.5^\circ$, (c) for HSM-paired rails, $\rho = 90.0^\circ$ and (d) for Hexaglide configuration

6. RESULTS AND DISCUSSION

In this work, workspace and dexterity analyses of a generic hexaslide manipulator was carried out. This generic model covers most of the specific configurations proposed by the researchers so far. Configurations include HSMs with both paired rails and unpaired rails. The results indicate that the workspace and dexterity strongly depend on the arrangement of rails. Effect of two important parameters related to configuration, gap between adjacent rails in case of hexaglide and inclination of rails in case of HSMs having slanted rails on workspace and dexterity was studied.

It was found that the HSM having slanted rails parallel by pairs offer maximum workspace. The optimum slanting angle was found to be in the vicinity of 43°. A maximum value of work volume index, found to be 0.231 i.e., workspace would be 23.1% of the machine size, and was offered by the same HSM having slanted rails parallel by pairs with a slant angle of 43°. But the dexterity offered by this configuration, however, is not optimum. The global dexterity index, in case of these HSMs with slanted rails parallel by pairs, ranges from 0.183 to 0.335 corresponding to 22.5° and 67.5° rail-inclinations respectively. In case of hexaglide configuration, maximum workspace volume is offered when the gap between adjacent rails is 0.102m. The results indicate that the workspace and dexterity strongly depend on the arrangement of rails i.e., gap between adjacent rails in case of hexaglide configuration and inclination of rails in case of HSMs with slanted rails has been established.

7. CONCLUSIONS

In this work, kinematic analyses of a class of parallel manipulators, namely, Hexaslides was carried-out. Various kinematic performance indices, namely, workspace volume, workspace volume index and global dexterity index of hexaslides having same foot print size were used to study different rail-arrangements. Influence of the gap between adjacent rails in case of hexaglide configuration and inclination of rails in case of slanted Configuration, on the performance measures was also presented. Strong dependence of workspace and dexterity on gap between adjacent rails and inclination of rails has been established.

8. FUTURE WORK

The present work can be extended to a generic HSM configuration and workspace and dexterity analyses for all possible tool orientations. There is also a need to study the influence of other design parameters such as leg-length, rail-length etc. to arrive at an optimum design configuration. However, one main concern, which needs to be addressed in extending the work, is to improve the computational efficiency in evaluating the performance indices.

REFERENCES

- [1] D.Stewan, "A platform with six degrees of freedom", *Proceedings Institution of Mechanical Engineers*, (Pan-I), vol. 180, no. 1S, 1965, pp. 371-386.
- [2] V.E.Cough and S.G.Whitehall, "Universal Tyre test machine", in *Proceedings of the 9th International Technical Conferences*, F.I.S.I.T.A., Institution of Mechanical Engineers, vol. 117, 1962, pp.117-135.
- [3] M.Honegger, A.Codourey and E.Burdet, "Adaptive control of the Hexaglide, a 6 DOF parallel manipulator", in *Proceedings of IEEE International Conference on Robotics and Automation*, Albuquerque, 1997, pp.543-548.
- [4] M.Suzuki, K.Watanabe, T.Shibukawa, T.Tooyama and K.H.Hoti, "Development of milling machine with parallel mechanism", *Toyota Technical Review*, vol. 47, no. 1, 1997, pp.125-130.
- [5] G.Pitschow and K.H.Wurst, "Systematic design of Hexapods and parallel link systems", *Annals of the CIRP*, vol. 46, no. 1, 1997, pp.291-291.
- [6] I.Kim, F.C.Park and J.M.Lee, "A new parallel mechanism Machine tool capable of five-face machining", *Annals of the CIRP*, ~01.48, no. 1, 1999, pp.337-340.
- [7] P.Wenger, C.Gosselin and B.Maille, "A Comparative Study of serial and parallel mechanism topologies for Machine tools", in *Proceedings of PKM'99, Milano*, 1999, pp. 23-32.
- [8] T.Treih and O.Zim, "Similarity laws of serial and parallel manipulators for Machine Tools", in *Proceedings of the 5th International Conference on Motion and Vibration Control - MOVIC'98*, Zurich, Aukt 25-28. (http://www.ifr.mavt.ethz.ch/movic98/proceedings/slc.pdf)
- [9] D.N.Centea, H.Lacheray, F.Audren, R.Teltz and M.A.Elbestawi, "Development of TIARA Hexapod-a Machine tool based on parallel kinematic SI-cNT-s", *Transactions of ASME Journal of Manufacturing Science and Engineering*, vol. 10, 1999, pp.869-878.
- [10] I.A.Bonev and J.Rp, "Workspace analysis of 6-PRRS parallel manipulator- based on the view space concept", in *Proceedings of the ASME Design Engineering Technical Conferences*, September 12-15, 1999, DETC99 IDAC-8647.
- [11] F.Xi, "A comparison Study on Hexapods with fixed-length legs", *International Journal of Machine Tools & Manufacture*, VOL 41, 2001, pp. 1735-1748.
- [12] I. Saliubury and J.Craig, "Aniculated Hands: force control and kinematic issues", *International Journal of Robotic Research*, vol.1, no. 1, 1982, pp.4-17.
- [13] T.Yoshikawa, "Fundamentals of robotics: analysis and control", PHI, MIT Press, 1998, pp.131.
- [14] P.Wenger and D.Chablat, "Design of a three-axis Isotropic parallel manipulator for machining applications: The Otrahaglid", in *Proceedings of the Workshop on Fundamental Issues and Future Research Directions for Parallel Mechanisms and Manipulators*, October 3-4, Quebec, Canada, 2002, pp. 16-24.
- [15] C.Cosselin and J.Angeles, "A global performance index for the kinematic optimization of robotic manipulators", *ASME International Journal of Mechanical Design*, vol. 113(3), 1991, pp.220-226.
- [16] Xin-Jun Liu, Zhen-Lin Jin and Feng Cao, "Optimum design of 3-DOF spherical parallel manipulators with respect to the conditioning and stiffness indices", *Mechanism and Machine Theory*, vol. 35, 2000, pp. 1257-1267.
- [17] G.N.Sandor, and A.C.Erdman, "Advanced Mechanism Design: Analysis and Synthesis", Prentice Hall, vol.2, 1988, pp.550-551.
- [18] Lung-Wen Tsai, "Robot Analysis?", John Wiley & Sons, Inc., 1999, pp 31-45.
- [19] J.P.Merlet, "Determination of 6D workspaces of Cough-Type parallel manipulator and comparison between different geometries", *The International Journal of Robotics & Research*, vol.18, no.9, 1999, pp.902-916.
- [20] O.Masory and J.Wang, "Workspace evaluation of Stewart platforms", *Advanced Robotics*, vol.9, no.4, 1995, pp.443-461.